Review

Reactive Cobalt–Oxo Complexes of Tetrapyrrolic Macrocycles and *N*-based Ligand in Oxidative Transformation Reactions

Atif Ali, Waseem Akram and Hai-Yang Liu *

Department of Chemistry, The Key Laboratory of Fuel Cell Technology of Guangdong Province, South China University of Technology, Guangzhou 510641, China; atifali.chemistry@gmail.com (A.A.); waseem66@163.com (W.A.)
* Correspondence: chhyliu@scut.edu.cn; Tel.: +86-020-2223-6805

check for updates

Abstract: High-valent cobalt–oxo complexes are reactive transient intermediates in a number of oxidative transformation processes e.g., water oxidation and oxygen atom transfer reactions. Studies of cobalt–oxo complexes are very important for understanding the mechanism of the oxygen evolution center in natural photosynthesis, and helpful to replicate enzyme catalysis in artificial systems. This review summarizes the development of identification of high-valent cobalt–oxo species of tetrapyrrolic macrocycles and *N*-based ligands in oxidation of organic substrates, water oxidation reaction and in the preparation of cobalt–oxo complexes.

1. Introduction

In biological systems, metalloenzymes, typically containing Mn, Fe and Cu centers, are known to catalyze a wide range of reactions including aliphatic and aromatic C–H hydroxylation, epoxidation, desaturation, and heteroatom (S, N or O) dealkylation or oxidation [1,2]. It is well known that iron-oxo species are the reactive oxidants in the catalytic cycle of heme [3] and non-heme iron enzymes [4]. Similarly, manganese–oxo complex has been suggested the key intermediate in oxygen-evolving center of photo-system II (PSII) [5–7]. The transition metal–oxo complexes of iron and manganese involved in artificial oxygen transfer and C–H bond activations reactions have been extensively reviewed [8–13]. Except for the early transition metal–oxo complexes, high-valent metal–oxo complexes of late transition metals, particularly cobalt–oxo complexes, are also highly reactive transient intermediates in cobalt-catalyzed C-H bond activation and O-O bond formation reactions [14–16], and they are considered to be more reactive then related iron-oxo species due to a weak metal–oxygen bond [17,18]. Currently, clean energy production by maneuvering natural photosynthesis in water oxidation reactions to develop artificial photosynthesis [19–21] for efficient water splitting is a hot topic of research [22–24]. In particular, the cobalt oxides are often used materials for water oxidation to generate molecular oxygen [25–28]. The high-valent cobalt–oxo complexes of *N*-based ligand can be implicated as reactive species in the O–O bond-forming event during water oxidation [29,30]. Furthermore, cobalt complexes based on tetrapyrrolic macrocycles are often used in mimicking the peroxidase-like activity for the selective oxidation of organic substrates via high-valent cobalt(IV)–oxo intermediates [31,32]. Obviously, in the study of the reactive oxidants in these catalytic reactions it is essential to provide insight into their mechanism of reaction, allowing us to probe the critical step in these challenging reactions. However, the isolation and identification of these transient intermediates is considerable challenge. The cobalt–oxo complexes are not stable because cobalt has large number of

d-electrons which produces strong electronic repulsion between the rich electron oxygen and cobalt center. Also, the strong oxidative environment will cause oxidative degradation of the ligand, making the high-valent cobalt–oxo complexes unstable. To reduce the electronic repulsion between cobalt and oxygen, and to avoid oxidative degradation, tetrapyrrolic macrocylces and *N*-based ligands with a different electronic environment were implemented to increase the stability of cobalt–oxo complexes (Figure 1). Mostly, these can only be characterized in situ by electron paramagnetic resonance (EPR) [33], X-ray absorption [34] and time-resolved Fourier-transform infrared (FT-IR) [16] spectroscopic methods. Computational studies were also carried out to understand the nature of species involved in water oxidation [35]. Recently, the isolation and/or identification of high-valent cobalt–oxo complexes has become a key topic in order to develop and understand the mechanism of artificial photosynthesis and to replicate enzymatic process in artificial reactions.
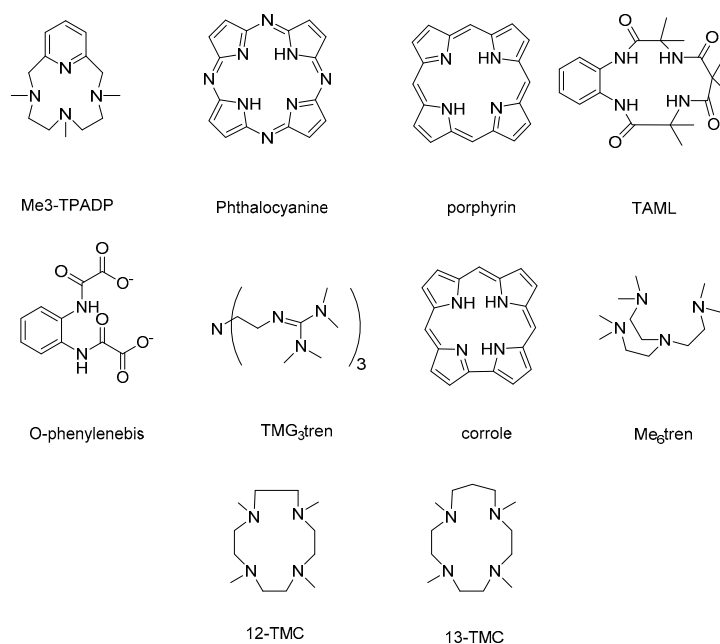
Figure 1. Some of the most used tetrapyrrolic macrocycles and *N*-based ligands used to stabilize high-valent cobalt–oxo complexes.

This review comprehends the high-valent cobalt–oxo complexes of tetrapyrrolic macrocycles and *N*-based ligands reported to date, along with outlooks in this intriguing research area. It has been divided into three sections: identification of cobalt–oxo species involved in oxidation of organic substrates; identification of cobalt–oxo species involved in heterogeneous and homogeneous water oxidation reactions; and preparation of high-valent cobalt–oxo complexes.

2. Cobalt–Oxo Species Involved in Oxidation of Organic Substrates

Cobalt–oxo species are involved in many of oxidative and C-H bond activation reactions. The ligands used to generate cobalt–oxo species play a key role in stabilizing cobalt–oxo species. Also, to mimic the enzymes-like environment, different types of support are used as protein backbone for example cellulosic fiber and multiwall carbon nanotubes. These supports cannot alter the reaction mechanism however, precisely control the generation of reactive intermediate, which also determines the activity, durability and stability of the complexes [36–38].

Nam et al. reported [39] the catalytic oxidation of alkene and alkane using cobalt-substituted polyoxotungstate and employed different oxidants such as iodosylbenzene, potassium monopersulfate and *m*-CPBA. Cobalt-substituted polyoxotungstate was proved to be a good catalyst. They proposed the involvement of different cobalt–oxo species with the different oxidants. Two possible species may form with iodosylbenzene, high-valent cobalt(V)–oxo 1 and cobalt–iodosylbenzene adduct 2

(Scheme 1). They suggested that complex 2 is responsible for oxygen transfer because cobalt cannot be obtained in +5 oxidation state. $KHSO_5$ and *m*-CPBA predict the involvement of cobalt(III)–oxygen adducts as oxygen transfer complex. Isotopically labeled water ($H_2^{18}O$) is a useful experimental tool to investigate the involvement of high-valent cobalt–oxo species in cobalt-mediated oxygen atom transfer reactions, but all the attempts to obtain ^{18}O-labeled products have failed. Furthermore, porphyrins are extensively used to get stable metal–oxo complexes [13]. Therefore, porphyrins with a different electronic environment were used to stabilize cobalt–oxo species [40,41]. Cobalt(IV)-oxo [40] and cobalt(IV)–oxo porphyrin radical [41] were proposed to be involved in C-H bond activation reaction. These species are quite reactive towards the oxidation of alkane and alcohol, respectively. However, there is no experimental evidence to support presence of cobalt–oxo species due to instability. Likewise, a cobalt(IV)–oxo species was reported [42], based on the tetraanionic cobalt(II) complex of (^{Br}HBA-Et)H_4, *N,N'*-(ethane-1,2-diyl)bis(5-bromo-2-hydroxybenzamide), that provides a strong ligand field. Consequently, this specie was stable enough to be characterized by EPR and ESI-MS spectroscopy analysis. Also, the presence of high-valent cobalt(IV)–oxo porphyrin was reported during the oxidation of alcohol to benzaldehyde by molecular oxygen in the presence of isobutyraldehyde, using bifunctional hybride catalyst originated from cobalt tetra(4-sulfonatophenyl)porphyrinate anion [43] and a cationic *meso*-tetrakis (1-methyl-4-pyridyl) cobalt porphyrin immobilized in montmorillonite interlayers [44]. The presence of a cobalt(IV)–oxo specie was predicted by an ^{18}O-labeled experiment of product [43]. The turnover frequency and catalytic yield was higher in the prior case. Later, the cobalt(IV)–oxo porphyrin was generated [45] by the oxidation of cobalt porphyrin Co(TPFPP)(CF_3SO_3) utilizing *m*-CPBA as oxidant in solvent mixture of CH_3CN and CH_2Cl_2. Incorporation of $H_2^{18}O$ in the catalytic oxidation demonstrated the presence of ^{18}O-labeled alcohol in the product, which is evidence for the presence of cobalt–oxo species. Furthermore, cobalt(V)=O and cobalt(IV)=O were generated [46] by the oxidation of a mononuclear non haem cobalt(III) [Co((bpc)Cl_2][Et_4N] (H_2bpc=4,5-dichloro-1,2-bis(2-pyridine-2-carboxamido)benzene) complex of a tetradentate ligand containing two deprotonated amide moieties with PhIO. Oxidation of the cobalt(III) complex generated cobalt acylperoxo intermediate, which on the heterolytic and homolytic cleavage of O-O bond generated respective cobalt(V)–oxo and cobalt(IV)–oxo species. These species are also not enough stable to be characterized spectroscopically. Similarly, a cobalt(IV)=O specie based on isoindole-core ligand was proposed [47] as a reactive intermediate, during the stereoselective oxidation of alkane using *m*-CPBA as oxidant. The kinetic isotopic effect and ^{18}O-labeled experiment predict the involvement of cobalt–oxo species. Recently, the involvement of a high-valent cobalt(IV)=O radical cation was proposed [48] during the reduction of O_2. The dianionic pentadentate ligand system based on bis-pyrazolyl diaryl borate arms attached to a 2,6-substituted pyridyl frame was used to stabilize the cobalt(IV)–oxo intermediate. Cobalt(IV)=O radical cation was generated by the cleavage of Co-O bond, and examined theoretically and experimentally. A density functional theory (DFT) calculation suggests the presence of maximum electron density at oxygen 70% with Co-O bond length of 1.67 Å.
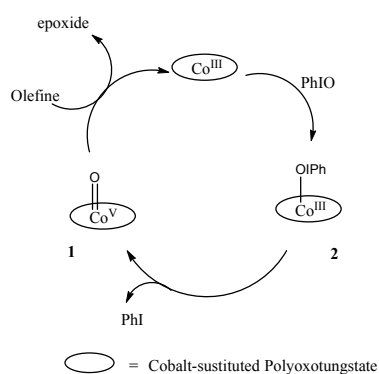
Scheme 1. Proposed mechanism for oxidation of alkene by cobalt polyoxotungstate using PhIO as oxidant [39].

Moreover, to mimic the enzyme activity for controllable catalytic oxidation, researchers made extensive efforts to develop and discover functional materials having properties intrinsic to enzymes. Many transition-metal complexes were prepared [49–51] to mimic the expected features of enzymes, such as selectivity and steric accessibility, but these do not present the said features due to the non-natural environment. A catalyst which is a replication of enzyme should possess a suitable cavity or cleft for accessibility of substrates and introduction of functional groups that act as active sites within the cavity [52,53]. Enzymatically inspired catalytic system was prepared by using cobalt tetraaminophthalocyanine (CoTAPc) as a catalyst supported by ordered-mesoporous-carbon (OMC) for controllable activation of hydrogen oxide (H_2O_2) to generate stable cobalt–oxo intermediate [32]. Ordered-mesoporous-carbon provides the steric environment for a substrate to attach with active sites and protects the active sites against the external interface. However, a disadvantage of hydrogen peroxide is the formation of hydroxyl radical that is highly reactive, so it decreases the selectivity. A fifth ligand dodecylbenzenesulfonate (LAS) is employed to inhibit the production of hydroxyl radical. This fifth ligand also helps to generate high-valent cobalt(IV)–oxo specie by heterolytic cleavage of peroxide O-O bond. The involvement of cobalt–oxo specie was corroborated by the results of semiempirical quantum-chemical PM6 calculations. Similarly, a modification in the tetrapyrrolic macrocycle of cobalt tetraaminophthalocyanine (CoTAPc) was made by the attachment of epoxy compound 2,3-epoxypropyl triethylammonium chloride (EPTAC), to obtain a new catalyst with positively charged quaternary ammonium salt chain (OMC-CoTAPc-EPTAC) [31]. The modified catalyst displays high catalytic activity especially for negatively charged substrates. The free radical trapping EPR analysis using 5,5-Dimethyl-1-pyrroline *N*-oxide (DMPO) as a free radical scavenger did not detect DMPO-·OH and DMPO-·OOH signal, ruling out the free radical type mechanism. That is why, the cobalt(IV)–oxo complex was proposed as a reactive intermediate due to the heterolytic cleavage of O-O bond of peroxide. Moreover, cellulosic fiber could play the role of the protein backbone in enzymes, providing an enzyme-like environment with enhanced regioselectivity to remove organic dyes and improve the stability of intermediate generated. A catalyst was developed based on cellulosic fiber-bonded cobalt phthalocyanine catalytic entity to activate hydrogen peroxide in order to generate cobalt–oxo specie [54]. The reaction channel was controlled by linear alkylbenzene sulfonate (LAS). High-valent cobalt(IV)–oxo specie **4** was generated by the heterolytic cleavage of peroxide O-O bond and homolytic cleavage generate cobalt(III)–oxo specie **3** (Figure 2).
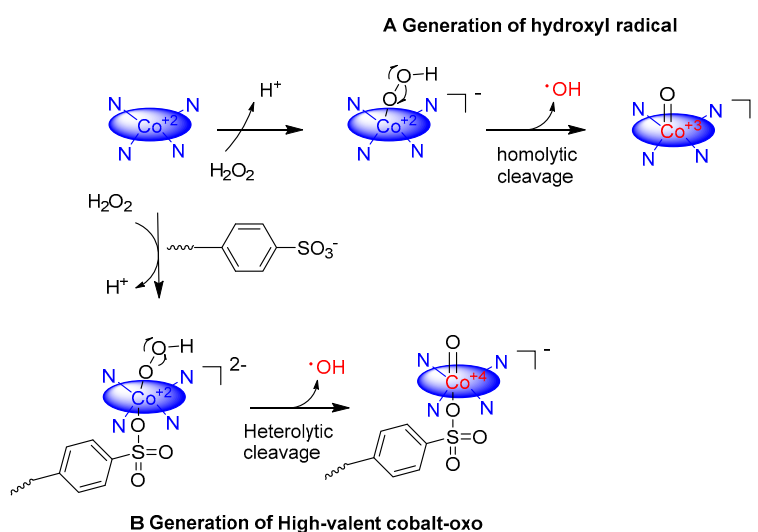

Figure 2. Possible pathway for the formation of active species in cellulosic fiber-bonded cobalt phthalocyanine (CoPc) H_2O_2 system. (**A**) Generation of hydroxyl radicals without ligand dodecylbenzenesulfonate (LAS) by the homolytic cleavage of the peroxide O-O bond; (**B**) Generation of cobalt–oxo with LAS by the heterolytic cleavage of the peroxide O-O bond [54].

The in situ X-band EPR analysis was conducted at room temperature in the presence of LAS demonstrating a signal at g_{eff} = 2.099 identifying the presence of Co^{IV} with spin state (S = $\frac{1}{2}$). Usually, metal–oxo species have been detected at low temperature [55,56]; a high oxidation state of $PcCo^{IV}$=O was observed at room temperature, presenting high stability of complex, auto-oxidation protected by cellulose matrix. Cellulosic fiber bonded cobalt phthalocyanine (CoPc) can also activate peroxymonosulfate [57]. The oxidation activity of catalyst is remarkably enhanced in the presence of bicarbonate ion (HCO_3^-) due to the generation of ($PcCo^{IV}$=O) by the heterolytic cleavage of O–O bond of peroxymonosulfate. Later, the same group [58] employed the multiwall carbon nanotubes (MWCNTs) as protein-like backbone anchored on cobalt phthalocyanine (CoPc) for peroxidase like activation of hydrogen peroxide. The anchoring of catalytic entity on MWCNTs decreases the diffusional mass transfer process (DMTP) and enhances the resistance of CoPc-MWCNTs oxidative decay. The introduction of linear alkylbenzene sulfonates (LAS) facilitates the heterolytic cleavage of O-O bond of peroxide to generate cobalt(IV)–oxo species. Furthermore, pyridine functionalized MWCNTs were produced and axially coordinated on the cobalt phthalocyanine (CoPc), generating a catalyst with increased catalytic activity and stability [59]. The heterolytic cleavage of O-O bond of hydrogen peroxide to produce cobalt(IV)–oxo without presence of any fifth ligand. The high-valent cobalt(IV)–oxo was analyzed by in situ ESI-MS and density functional theory. The DFT calculated bond length of Co-O bond is 1.806 Å and unpaired electron spin populations are mainly on the oxygen. Cobalt(IV)–oxo **5** was generated at pH = 10, the catalytic cycle starts with the coordination of OOH^- with Co^{II}, and the heterolytic cleavage of O-O occurs with the release of OH^- (Figure 3a). Moreover, non-haem cobalt(III) oxamate anion could also be used to stabilize high-valent cobalt(IV)–oxo species [60]. The oxidation of industrial contaminants was reported [61] by immobilizing non haem cobalt(III) complex [Co^{III}(opbaX)]$^-$ (opbaX = 4-X-o-phenylenebis(oxamate) on pyridine-modified MWCNTs, where pyridine acts as a fifth ligand. Similarly, cobalt(III) complexes of [Co^{III}(opbaX)]$^-$ (opbaX = 4-X-o-phenylenebis(oxamate), X = H, NO_2, CH_3) with different substituents was reported [62] for accelerating heterolytic cleavage of hydrogen peroxide to imitate the essential and general principle of natural enzymes without using any fifth ligand (Figure 3b). An ESI-MS and EPR trapping technique revealed the presence of cobalt(IV)–oxo reactive specie. The generation of cobalt–oxo species depends on the electronic environment of substituent. In Scheme 2 pathway (b) the electron rich cobalt complex favors the homolytical cleavage of the hydroperoxide O-O bond while the electron deficiency favors the heterolytic cleavage with generation of (Co^{IV}=O)**10**. The tendency of generation of (Co^{IV}=O) was in order **8** > **7** > **9**. Density functional theory also demonstrated that electron withdrawing group helps in pulling electron and lowering the corresponding energy levels. Keeping in mind the concept of the "oxo wall" [63], another pathway (a) also proposed, heterolytic cleavage of O-O generate the ligand based radical intermediate OH–Co^{III}(opbaX)**11**, in which ligand transfers one electron to cobalt and cobalt transfers it to oxygen.

Our group recently [64] reported the catalytic oxidation of alkene using four cobalt(III) corroles of different electronic environment F_0C-Co, F_5C-Co, F_{10}C-Co and F_{15}C-Co employing various oxidants. The in situ ESI HR-MS analysis of styrene oxidation with $KHSO_5$ predicts the presence of high-valent cobalt(V)–oxo complex as active intermediate. The in situ X-band CW EPR analysis revealed a signal at g = 2.0135 for the presence of cobalt–oxo specie.
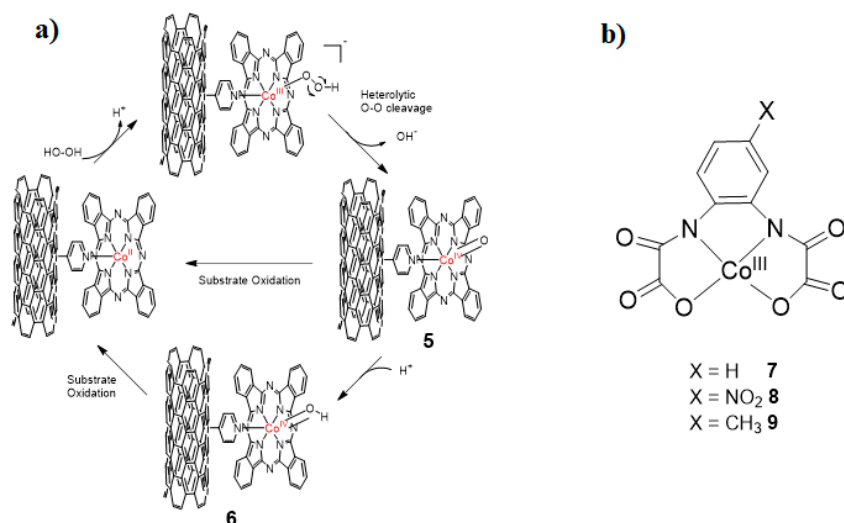
Figure 3. (**a**) Proposed mechanism of activation of H_2O_2 catalyzed by CoPc-PyMWCNTs for oxidation of substrates at pH = 10 [59]. (**b**) structures of cobalt(III) complexes involved in the activation hydrogen peroxide [62].
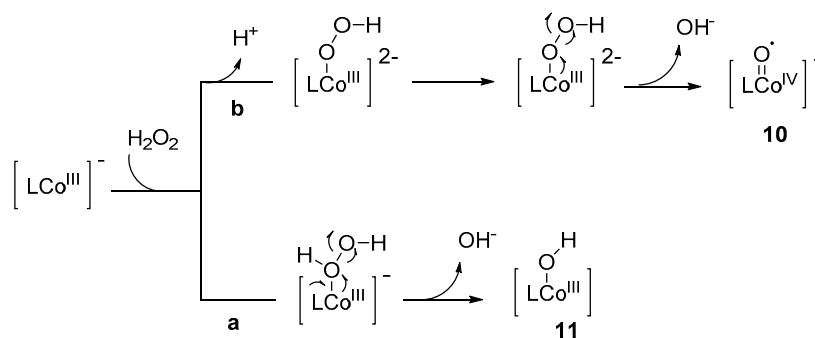

Scheme 2. Proposed mechanism for the formation of cobalt–oxo species (L = bis-benzoamido) [60].

3. Cobalt–Oxo Species Involved in Water Oxidation Reaction

Water oxidation is a process that involved the four-electron-four-proton oxidation of water to evolve O_2. In natural photosynthesis, sunlight is converted to chemical energy by the oxidation of water [20]. As a consequence, understanding nature's water oxidation mechanism in photosystem II has been the focus of research for the development of artificial water oxidation catalyst. The development of efficient water oxidation catalysts with minimal cost is a challenge [65–68]. Various water oxidation catalysts were developed to understand the O-O bond formation event in natural photosynthesis to evolve oxygen. Cobalt is the most abundant and cheap earth metal. Cobalt oxide materials are among the most promising catalyst for water oxidation [69–71] and cobalt–oxo species are involved in the O-O forming event of water oxidation.

Frei et al. reported [16] the photocatalytic water oxidation using cobalt oxide. The water oxidation was carried out in the presence of photosensitizer $[Ru(bpy)_3]^{2+}$ (bpy = 2,2′-bipyridine) that creates a hole and $S_2SO_8^{-2}$ as an electron acceptor. The FT–IR characterization revealed the involvement of two intermediates with absorption band at 1013 cm^{-1} and 840 cm^{-1}. The band at 1013 cm^{-1} was assigned to Co(III)OO (fast site) group with a neighboring hydroxyl group. Incorporation of $H_2{}^{18}O$ shifts the peaks at 995 cm^{-1} and 966 cm^{-1}. The shifting of frequency agrees well with the presence of superoxide moiety on a metal-oxide surface [72,73]. The superoxide surface intermediate causes the three-electron water oxidation. The band at 840 cm^{-1} was assigned to Co^{IV}=O (slow site) surface species. No change in the spectrum was observed by the incorporation of $H_2{}^{18}O$, ruling out the presence of any peroxide intermediate. From the mechanistic point of view, Co^{IV}=O was

generated by the oxidation of surface group Co(III)–OH. At the fast site catalytic species, catalytic turn over frequency is at least 10 times more than slow site catalytic species, because it has no neighbor hydroxyl group. Furthermore, Stahl et al. reported [74] the water oxidation employing cobalt oxide as an electrocatalyst, and proposed the involvement of (Co^{IV}-O) as reactive specie. The EPR analysis with signals at g-values 2.59, 2.17 and 1.99 revealed the presence of multiple paramagnetic species during water oxidation, possibly arising from (Co^{IV}-O) sites in the catalyst with a different coordination environment. The mechanism of water oxidation is pH dependent, at acidic pH homogeneous catalysis leading to H$_2$O$_2$ production, while at pH above 3.5 heterogeneous catalysis takes place, generating O$_2$ from four-electron water oxidation (Scheme 3). The oxidation of **12** produced **14** (**12**→**13**→**14**) corresponds to a 3H$^+$/e$^-$ process. Subsequently, 1e$^-$ oxidation generated specie **15** corresponding to 7H$^+$/3e$^-$ process. Further, oxidation of **15** afforded **16**. A key step to evolve oxygen is the nucleophilic attack of water at **16** to produce **17** [75–77]. Under the acidic pH, the PCET-mediated formation of **11** was prevented (Scheme 3). The oxidation of **10** produced **18** that dissolve from surface. The intermediate specie **18** invoked the homogeneous oxidation of water to H$_2$O$_2$ [78]. Similarly, bridging cobalt(IV)–oxo [79] and terminal cobalt(IV)–oxo radical [80] species were proposed as reactive catalytic sites for water oxidation, employing amorphous cobalt oxide. X-ray absorption near the edge provides the insight that the generation of high-valent (Co^{IV}-O) depended on the potential applied and pH. The edge position of the spectra was taken at pH = 7 and pH = 9 differs by about 1.0 eV by keeping potential constant at 0.95 V, and edge position of the spectra were taken at pH = 7 by increasing electrode potential from 0.95 to 1.34 V differs by about 1.2 eV [79]. However, the study of cobalt–oxo species involved in water oxidation was difficult because in oxygen evolving catalysis (OEC), large number of spectroscopically active backgrounds species are present which limits their detection and characterization.
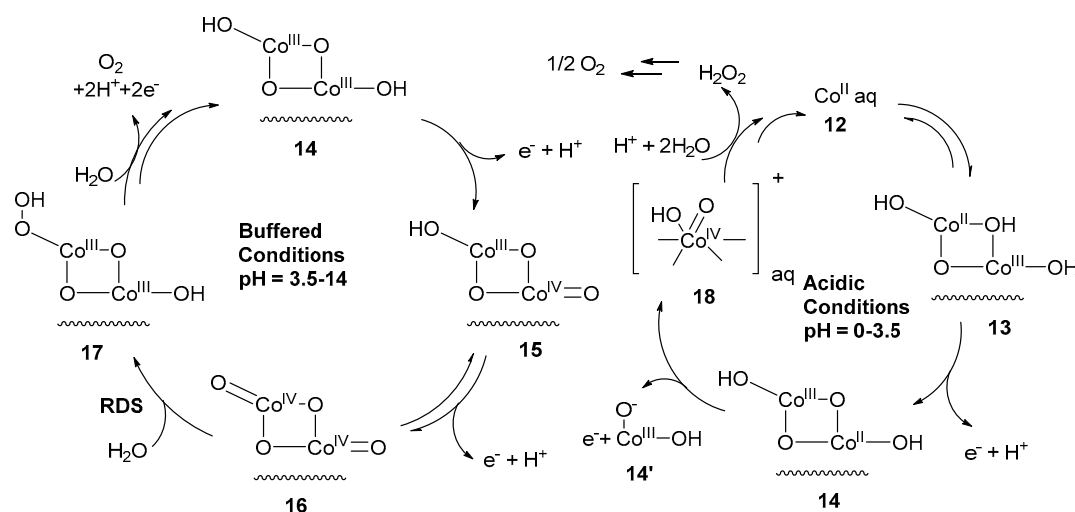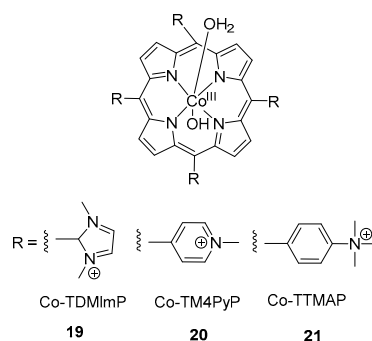

Scheme 3. Mechanism for oxidation of water by cobalt oxide under acidic and basic conditions [74].

Consequently, suitable catalysts to reduce background active species are needed to design. *N*-based ligands have attractive properties to be used as homogenous molecular water oxidation catalysts [81]. Recently, a significant number of catalysts are developed based on single site and multinuclear transition metal including Mn, Fe, Co, Cu, Ru and Ir [82–87]. The biggest challenge is to find a suitable coordination environment because the metal–ligand bond opposite a metal–oxygen bond can be compromised at higher redox level leading the catalyst to be susceptible to degradation [88]. So, single site *N*-based ligand homogeneous catalysts of cobalt were developed utilizing stable pentadentate ligand environment of 2,6-(bis(bis-2-pyridyl)methoxy-methane)-pyridine [89] and 6-(bis(bis-2-pyridyl)-methoxymethane)pyridine [30] for water oxidation. The electrochemical studies revealed that over pH range 7.6–10.3 an oxidation event was observed at +1.43 V vs. NHE corresponding

to $[Co^{IV}–OH]^{3+}/[Co^{III}–OH]^{2+}$ with significant rise in current. This signal is not classified as PCET because $E_{1/2}$ is static over this pH range. A pH dependent step was observed at pH > 10.3 corresponding to $[Co^{IV}=O]^{2+}/[Co^{III}–OH]^{2+}$ which is consistent with PCET. High-valent $[Co^{IV}=O]^{2+}$ species evolves O_2 by the nucleophilic attack of H_2O [89,90]. An alternative pathway proposed that the attack of OH- at $[Co^{IV}–OH]^{3+}$ in the rate determining step will evolve O_2 [30]. Likewise, $[Co^{IV}-O]$ specie was proposed as reactive intermediate during water oxidation at basic pH using cobalt-porphyrins as catalyst [91]. Similarly, Groves and Wang reported [92] the single site homogeneous water oxidation catalyst, employing a series of cobalt porphyrins **19**, **20** and **21** (Scheme 4). A high-valent Co^{IV}-porphyrin cation radical acts as reactive intermediate. The electrochemical experiment provides the evidence for the formation of high-valent $Co^{IV}–O$ specie. The redox event at 250 mV vs. Ag/Cl reference represents the resting state of catalyst $H_2O–Co^{III}–OH$ **23**. The observed anodic features at ~1 V demonstrates the oxidation of Co^{III} porphyrin to Co^{III} porphyrin radical cation (+P-Co^{III}–OH) **24**. As first oxidation occurred before the onset potential of WOC catalytic current, so +P–Co^{III}–OH is not the reactive oxidant in this system. The second oxidation at 1320 mV generates a reactive high-valent $Co^{IV}–O$ porphyrin radical cation **25**. The key step for O-O bond formation is the nucleophilic addition of H_2O to +P–Co^{IV}–O **25** to form Co-hydroperoxo or peroxo which further oxidized to evolve O_2 as shown in Scheme 5. Likewise, photo-induced generation of $Co^{IV}=O$ as active oxidant for the water oxidation was reported [93] based on a cobalt(II) complex of salophen ligand. Moreover, a high-valent $Co^{IV}O$ complex isoelectronic to $Co^{V}O$ was reported [29] to act as active specie to generate O_2 based on a cobalt(III) complex of *N*-based ligand bTAML (bTAML = biuret-modified tetraamidomacrocyclic) ligands. The complex $[Co(O)(bTAML)]^{1-}$ cannot be characterized by spectroscopic techniques due to the non-innocent nature of the ligand except UV-vis spectra. The same specie was generated by the one electron oxidation using cerium ammonium nitrate in the presence of $ZnCl_2$. The HR-MS analysis revealed the m/z = 497.026 corresponding to $[Co^{IV}(O)(Zn)(bTAML)(H^+)]$. Further, Nocera et al. reported [94] the dicobalt oxidized site $Co(III)_2Co(IV)_2$ during water oxidation using cobalt cubane modified by pyridine ligands that can stabilize tetracobalt core. This pyridine-modified cobalt cubane has molecular nature and termed as molecular cubane. Electrochemical investigation demonstrated two reversible oxidation events at $E_0(1)$ = 0.3 V and $E_0(2)$ = 1.25 V corresponding to $Co(III)_3(IV)/Co(III)_4$ and $Co(III)_2(IV)_2/Co(III)_3(IV)$. X-ray absorption spectroscopy also confirms the presence of $Co(III)_2(IV)_2$ specie. The adjacent terminal $Co^{IV}=O$ species in cubane provide a site for direct O–O bond formation by radical coupling to evolve O_2. Likewise, the proton-coupled electron transfer generation of $(Co^{IV}-O)$ was also reported [95] using molecular model cubane, $[Co_4O_4(CO_2Me_2)_2(bpy)_4]$. Furthermore, molecular cobalt cubane $Co_4O_4(OAc)_4py_4$ **26** [96] and a series of modified molecular cobalt cubane with electron rich and electron poor groups [97] were reported to understand the nature of high-valent cobalt–oxo species involved in the water oxidation reaction. The electrochemical studies of **26** revealed the presence of only one fully redox couple from pH 4 to pH 10 at $E_{1/2}$ = 1.25 V corresponding to $Co(III)_4/Co(III)_3(IV)$ redox. The increase of pH to 12 produced a significant anode wave current and bubble formation, consistent with the oxidation of hydroxide to oxygen. No change in the current intensity was observed in the presence of EDTA, ruling out the possibility of heterogeneous water oxidation due to the presence of Co^{II} oxide. The ESI-MS analysis by incorporating 97% enriched $Na^{18}OH$ observed the presence of 90% $^{36}O_2$. No evidence for the exchange of ^{18}O-oxygen between **26** revealing that only terminal oxo/hydroxide specie was involved in O-O bond formation. The reaction of protonated **26+** and hydroxide showed the importance of the cobalt(IV) oxidation state in O_2 formation. The generation of cobalt(V)=O **26(O)** was proposed by PCET before the evaluation of O_2 as shown in Scheme 6 [96]. The protonated **26+** reacts with hydroxide ion to produce **26(O)−** which further oxidized to cobalt(V)=O **26(O)**. The specie **26(O)** had acted as reactive intermediate to evolve O_2. Involvement of high-valent cobalt(V)=O complex during water oxidation was also theoretically proposed [98–101]. Corroles are analogous of porphyrin which have one carbon less than porphyrin and can stabilize metals in a higher oxidation state. A high-valent $Co^V=O$ specie suggested [102] to act as reactive specie during water oxidation by using series of cobalt

corroles with different axial ligand. Electrochemical study of cobalt corroles represent two reversible oxidation events at $E_{1/2} = 0.75$ and $E_{1/2} = 1.32$ V vs. NHE corresponding to Co^{IV}/Co^{III} and Co^{V}/Co^{IV} redox couples, respectively. Nucleophilic attack of the water at Co-O bond to generate Co-hydroperoxo specie is the key step to evolve O_2. Cobalt corroles with electron-donating ligands are more reactive because it causes the Co-O bond to be weaker and nucleophilic attack become easier.

Scheme 4. Molecular structures of cobalt porphyrins employed as water oxidation catalyst.
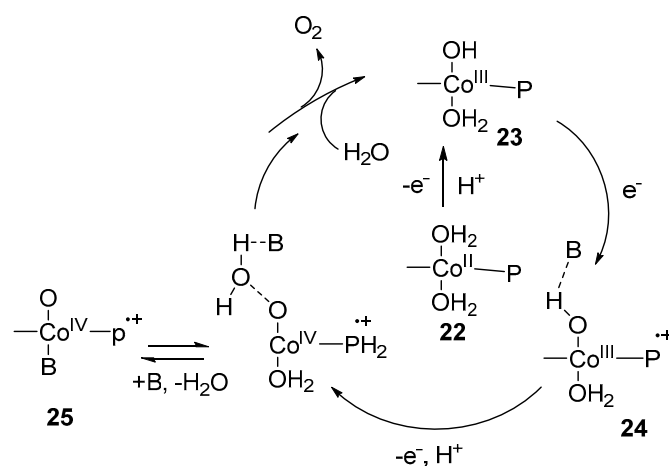
**Scheme 5.** Proposed mechanism of water oxidation catalyzed by cobalt porphyrins [92].
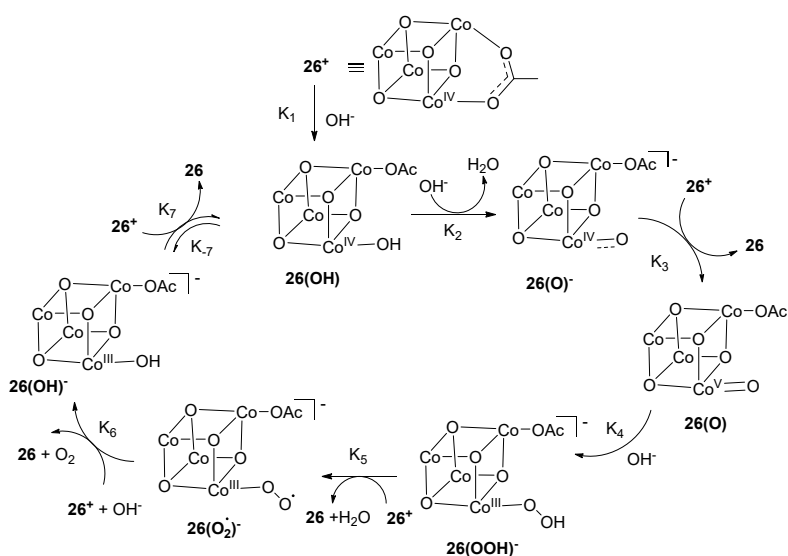
Scheme 6. Generation of high-valent Co^V=O **26(O)** during water oxidation by molecular cobalt cubane $Co_4O_4(OAc)_4py_4$ [96].
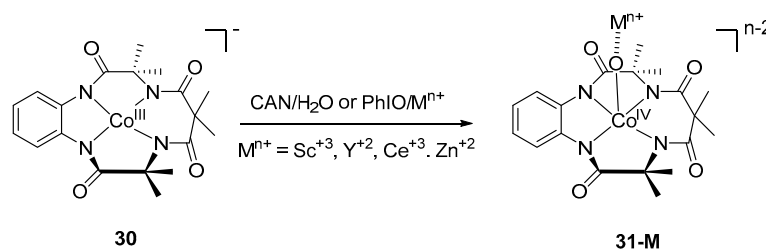
4. Preparation of Cobalt–Oxo Complexes

The isolated preparation of cobalt–oxo complexes have two major problems (1). Ligands used to stabilize cobalt–oxo complexes are prone to oxidation (2). Electronic repulsion forces between the d-electron of cobalt and electron of the oxygen. Chemists are focusing on how to overcome these problems to prepare cobalt–oxo complexes.

Ray et al. reported [103] the first preparation and isolation of terminal cobalt(IV)–oxo complex using the *N*-based tetradentate tripodal ligand TMG$_3$tren (tris[2-(*N*-tetramethylguanidyl)ethyl]amine). The {Co-O} unit was stabilized by the Lewis acid interaction with Sc^{+3} ion, generating {Co-O-Sc}$^{+3}$ unit. The complex **29** was obtained by two electron oxidation of **27**-OTf in the presence of Sc(OTf)$_3$ (Scheme 7). The complex **29** was characterized by electrospray mass spectrum, EPR and X-ray absorption spectroscopy, and was reactive towards oxidation of triphenylphosphine and dihydroanthracene. The same group two years later reported [104] the square pyramidal cobalt(IV)–oxo with enhanced stability based on the tetraamido macrocyclic ligand (TMAL). The electrochemical study of **30** gave a reversible oxidation peak at 1.00 V vs. a saturated colomel electrode. This reversible oxidation peak suggests that Co^{IV} state is thermally and kinetically accessible. The one electron oxidation of **30** in the presence of cerium ammonium nitrate (CAN) afforded a blue-colored complex **31**-Ce with a half-life of 20 min. This blue complex can also be obtained by the oxidation of **30** with PhIO in the presence other redox-inactive metals like Sc^{+3}, Y^{+3} and Zn^{+2} (Scheme 8). The complex **31-M** was characterized by cold-spray ionization time-of-flight mass spectrometry (CSI-TOF MS), X-band EPR spectrum, and X-ray absorption spectroscopy. All attempts to obtain resonance Raman spectrum have failed. The **31-Sc** complex demonstrated high reactivity in the hydrogen abstraction reaction and oxygen atom transfer reactions. The first fully spectroscopically characterized high-valent Cobalt(IV)–oxo complex **33** was generated [105] by the two electron oxidation of a cobalt complex of 13-TMC (2 mM) **32** by PhIO (3 equiv.) following conventional method in the presence of triflic acid (CF$_3$SO$_3$H, HOTf; 1.2 equiv.) in acetone (Scheme 9). The transient complex had a half-life of 3 h and was characterized by CSI-TOF MS, EPR and X-ray absorption spectroscopy. Resonance Raman spectroscopy considered as authentic technique to confirm the presence of metal–oxo complex [106,107]. The resonance Raman spectrum of **33** showed a band at 770 cm^{-1} which shifts to 736 cm^{-1} upon ^{18}O-labelling of **33**. Recently, preparation of Co^{III}≡O complex was reported [108] by using tris-(imidazol-2-ylidene)borate ligand PhB(tBuIm)$_3{}^-$. This complex was characterized by infrared (IR) and X-ray diffraction (XRD) spectroscopy. The length of Co-O bond determined by XRD was 1.68 Å. DFT calculations revealed two Co-O π* interactions with highest lying d$_{xz}$ and d$_{yz}$ orbitals. These orbitals support the presence of two π-bonds. This complex was thermodynamically unstable with half-life of 8 h.
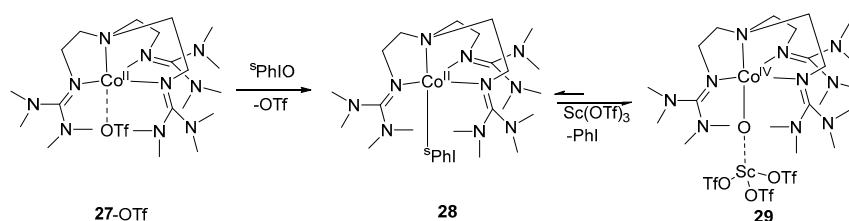
Scheme 7. Preparation of high-valent {Co^{IV}-O-Sc^{3+}} complex **29**.

Scheme 8. Oxidation of complex **30** to **31-M** by CAN/H$_2$O or PhIO/M^{n+}.
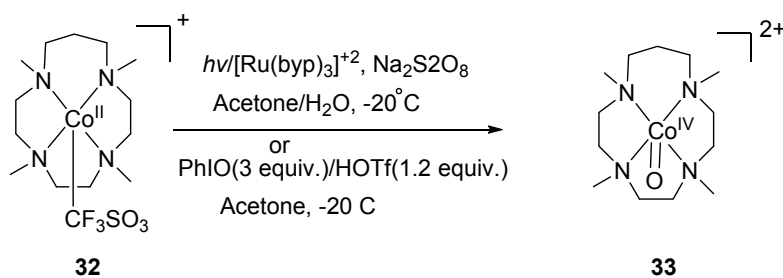
Scheme 9. Preparation of a mononuclear non-haem cobalt(IV)–oxo complex [(13-TMC)Co^{IV}(O)]$^{2+}$.

5. Summary and Outlook

High-valent cobalt–oxo complexes are implicated as key intermediates in many of the oxidative transformation reactions and the water oxidation process. Identification of cobalt–oxo species in water-splitting reactions have been extensively studied. However, the transient nature of cobalt–oxo complexes limits their characterizations to in situ EPR, XAS and mass spectroscopy. Although different strategies, such as using ligands with different electronic environments or MWCNT supports, have been adopted to stabilize cobalt–oxo complexes, until now only one example of Raman characterization for cobalt (IV)=O complex using 1,4,7,10-tetramethyl-1,4,7,10-tetraazacyclotridecane ligand has been available. The isolation and identification of high valent cobalt–oxo species remains a great challenge. The design of a suitable *N*-based ligand which can stabilize coordinated cobalt atom in high oxidation might be the key step for the preparation of higher valent cobalt–oxo complexes, which will allow the full characterization and "slow motion picture" study of the factors controlling its reactivity.

Author Contributions: H.-Y.L. coordinated the whole work and provided technical guidance. A.A. and W.A. collected the references and wrote the paper.

Conflicts of Interest: The authors declare no conflict of interest.

Abbreviations

TPFPP	*Meso*-tetrakis(pentafluorophenyl)porphinato dianion
CoTAPc	cobalt tetraaminophthalocyanine
EPTAC	2,3-epoxypropyl triethylammonium chloride
Pc	Phthalocyanine
TAPc	Tetraaminophthalocyanine
MWNCTs	Multiwall carbon nanotubes
DMPO	5,5-Dimethyl-1-pyrroline *N*-oxide
F$_0$C-Co	Co(III) complex of 5,10,15-triphenylcorrole
F$_5$C-Co	Co(III) complex of 5,15-bis(phenyl)-10-(pentafluorophenyl)corrole
F$_{10}$C-Co	Co(III) complex of 5,15-bis(pentafluorophenyl)-10-phenylcorrole
F$_{15}$C-Co	Co(III) complex of 5,10,15-tris(pentafluorophenyl)corrole
TMG$_3$tren	(tris[2-(*N*-tetramethylguanidyl)ethyl]amine)
^{s}PhIO	2-(*tert*-butylsulfonyl)iodosylbenzene
TMAL	Tetraamido macrocyclic ligand
13-TMC	1,4,7,10-tetramethyl-1,4,7,10-tetraazacyclotridecane
Co-TDMImP	Co(III) complex of 5,10,15,20-tetrakis(1,3-dimethylimidazolium-2-yl)porphyrin
Co-TM4PyP	Co(III) complex of 5,10,15,20-tetrakis(*N*-methylpyridinium-4-yl)porphyrin
Co-TTMAP	Co(III) complex of 5,10,15,20-tetrakis(*N,N,N*-trimethylanilinium-4-yl)porphyrin

References

1. Sono, M.; Roach, M.P.; Coulter, E.D.; Dawson, J.H. Heme-containing oxygenases. *Chem. Rev.* **1996**, *96*, 2841–2888. [CrossRef] [PubMed]

2. Meunier, B.; de Visser, S.P.; Shaik, S. Mechanism of oxidation reactions catalyzed by cytochrome p450 enzymes. *Chem. Rev.* **2004**, *104*, 3947–3980. [CrossRef] [PubMed]

3. Van Eldik, R. Fascinating inorganic/bioinorganic reaction mechanisms. *Coord. Chem. Rev.* **2007**, *251*, 1649–1662. [CrossRef]

4. Costas, M.; Mehn, M.P.; Jensen, M.P.; Que, L. Dioxygen activation at mononuclear nonheme iron active sites: Enzymes, models, and intermediates. *Chem. Rev.* **2004**, *104*, 939–986. [CrossRef] [PubMed]

5. Umena, Y.; Kawakami, K.; Shen, J.-R.; Kamiya, N. Crystal structure of oxygen-evolving photosystem II at a resolution of 1.9 Å. *Nature* **2011**, *473*, 55–60. [CrossRef] [PubMed]

6. Mullins, C.S.; Pecoraro, V.L. Reflections on small molecule manganese models that seek to mimic photosynthetic water oxidation chemistry. *Coord. Chem. Rev.* **2008**, *252*, 416–443. [CrossRef] [PubMed]

7. McEvoy, J.P.; Brudvig, G.W. Water-splitting chemistry of photosystem II. *Chem. Rev.* **2006**, *106*, 4455–4483. [CrossRef]

8. Rebelo, L.S.; Silva, M.A.; Medforth, J.C.; Freire, C. Iron(III) fluorinated porphyrins: Greener chemistry from synthesis to oxidative catalysis reactions. *Molecules* **2016**, *21*. [CrossRef]

9. Pereira, F.C.; Simões, M.M.; Tomé, P.J.; Almeida Paz, A.F. Porphyrin-based metal-organic frameworks as heterogeneous catalysts in oxidation reactions. *Molecules* **2016**, *21*. [CrossRef]

10. de Visser, S.P.; Rohde, J.-U.; Lee, Y.-M.; Cho, J.; Nam, W. Intrinsic properties and reactivities of mononuclear nonheme iron–oxygen complexes bearing the tetramethylcyclam ligand. *Coord. Chem. Rev.* **2013**, *25*, 381–393. [CrossRef]

11. Krebs, C.; Galonić Fujimori, D.; Walsh, C.T.; Bollinger, J.M. Non-heme Fe(IV)-oxo intermediates. *Acc. Chem. Res.* **2007**, *40*, 484–492. [CrossRef]

12. Abu-Omar, M.M.; Loaiza, A.; Hontzeas, N. Reaction mechanisms of mononuclear non-heme iron oxygenases. *Chem. Rev.* **2005**, *105*, 2227–2252. [CrossRef] [PubMed]

13. Baglia, R.A.; Zaragoza, J.P.T.; Goldberg, D.P. Biomimetic reactivity of oxygen-derived manganese and iron porphyrinoid complexes. *Chem. Rev.* **2017**, *117*, 13320–13352. [CrossRef] [PubMed]

14. Fukuzumi, S.; Mandal, S.; Mase, K.; Ohkubo, K.; Park, H.; Benet-Buchholz, J.; Nam, W.; Llobet, A. Catalytic four-electron reduction of O_2 via rate-determining proton-coupled electron transfer to a dinuclear cobalt-μ-1,2-peroxo complex. *J. Am. Chem. Soc.* **2012**, *134*, 9906–9909. [CrossRef] [PubMed]

15. Pfaff, F.F.; Heims, F.; Kundu, S.; Mebs, S.; Ray, K. Spectroscopic capture and reactivity of S = 1/2 nickel(III)-oxygen intermediates in the reaction of a Ni(II)-salt with mCPBA. *Chem. Commun.* **2012**, *48*, 3730–3732. [CrossRef] [PubMed]

16. Zhang, M.; de Respinis, M.; Frei, H. Time-resolved observations of water oxidation intermediates on a cobalt oxide nanoparticle catalyst. *Nat. Chem.* **2014**, *6*, 362–367. [CrossRef]

17. Pierpont, A.W.; Cundari, T.R. Computational study of methane C-H activation by first-row late transition metal L(n)M=E (M: Fe, Co, Ni) complexes. *Inorg. Chem.* **2010**, *49*, 2038–2046. [CrossRef]

18. Limberg, C. Was ist wirklich nötig, um Komplexe später Übergangsmetalle mit terminalen oxo-liganden zu stabilisieren? *Angew. Chem.* **2009**, *121*, 2305–2308. [CrossRef]

19. Cox, N.; Pantazis Dimitrios, A.; Neese, F.; Lubitz, W. Artificial photosynthesis: Understanding water splitting in nature. *Interface Focus* **2015**, *5*, 20150009. [CrossRef]

20. Yamada, T.; Domen, K. Development of sunlight driven water splitting devices towards future artificial photosynthetic industry. *ChemEngineering* **2018**, *2*, 36. [CrossRef]

21. Young, K.J.; Brennan, B.J.; Tagore, R.; Brudvig, G.W. Photosynthetic water oxidation: Insights from manganese model chemistry. *Acc. Chem. Res.* **2015**, *48*, 567–574. [CrossRef] [PubMed]

22. Yin, Q.; Tan, J.M.; Besson, C.; Geletii, Y.V.; Musaev, D.G.; Kuznetsov, A.E.; Luo, Z.; Hardcastle, K.I.; Hill, C.L. A fast soluble carbon-free molecular water oxidation catalyst based on abundant metals. *Science* **2010**, *328*, 342–345. [CrossRef] [PubMed]

23. Duan, L.; Bozoglian, F.; Mandal, S.; Stewart, B.; Privalov, T.; Llobet, A.; Sun, L. A molecular ruthenium catalyst with water-oxidation activity comparable to that of photosystem II. *Nat. Chem.* **2012**, *4*, 418. [CrossRef] [PubMed]

24. Smith, R.D.L.; Prévot, M.S.; Fagan, R.D.; Zhang, Z.; Sedach, P.A.; Siu, M.K.J.; Trudel, S.; Berlinguette, C.P. Photochemical route for accessing amorphous metal oxide materials for water oxidation catalysis. *Science* **2013**, *340*, 60–63. [CrossRef]

25. Kanan, M.W.; Nocera, D.G. In situ formation of an oxygen-evolving catalyst in neutral water containing phosphate and Co^{2+}. *Science* **2008**, *321*, 1072–1075. [CrossRef] [PubMed]

26. Jiao, F.; Frei, H. Nanostructured cobalt oxide clusters in mesoporous silica as efficient oxygen-evolving catalysts. *Angew. Chem. Int. Ed.* **2009**, *48*, 1841–1844. [CrossRef]

27. Esswein, A.J.; McMurdo, M.J.; Ross, P.N.; Bell, A.T.; Tilley, T.D. Size-dependent activity of Co_3O_4 nanoparticle anodes for alkaline water electrolysis. *J. Phys. Chem. C* **2009**, *113*, 15068–15072. [CrossRef]

28. Hans Wedepohl, K. The composition of the continental crust. *Geochim. Cosmochim. Acta* **1995**, *59*, 1217–1232. [CrossRef]

29. Das, D.; Pattanayak, S.; Singh, K.K.; Garai, B.; Sen Gupta, S. Electrocatalytic water oxidation by a molecular cobalt complex through a high valent cobalt oxo intermediate. *Chem. Commun.* **2016**, *52*, 11787–11790. [CrossRef] [PubMed]

30. Wasylenko, D.J.; Palmer, R.D.; Schott, E.; Berlinguette, C.P. Interrogation of electrocatalytic water oxidation mediated by a cobalt complex. *Chem. Commun.* **2012**, *48*, 2107–2109. [CrossRef]

31. Chen, Y.; Gu, Y.; Li, N.; Lu, W.; Chen, W. Efficient oxidative removal of organic pollutants by ordered mesoporous carbon-supported cobalt phthalocyanine. *J. Nanomater.* **2016**, *2016*, 27. [CrossRef]

32. Li, N.; Lu, W.; Pei, K.; Yao, Y.; Chen, W. Ordered-mesoporous-carbon-bonded cobalt phthalocyanine: A bioinspired catalytic system for controllable hydrogen peroxide activation. *ACS Appl. Mater. Interfaces* **2014**, *6*, 5869–5876. [CrossRef] [PubMed]

33. McAlpin, J.G.; Surendranath, Y.; Dincă, M.; Stich, T.A.; Stoian, S.A.; Casey, W.H.; Nocera, D.G.; Britt, R.D. EPR evidence for Co(IV) species produced during water oxidation at neutral pH. *J. Am. Chem. Soc.* **2010**, *132*, 6882–6883. [CrossRef] [PubMed]

34. Hadt, R.G.; Hayes, D.; Brodsky, C.N.; Ullman, A.M.; Casa, D.M.; Upton, M.H.; Nocera, D.G.; Chen, L.X. X-ray spectroscopic characterization of Co(IV) and metal–metal interactions in Co_4O_4: Electronic structure contributions to the formation of high-valent states relevant to the oxygen evolution reaction. *J. Am. Chem. Soc.* **2016**, *138*, 11017–11030. [CrossRef] [PubMed]

35. Retegan, M.; Krewald, V.; Mamedov, F.; Neese, F.; Lubitz, W.; Cox, N.; Pantazis, D.A. A five-coordinate Mn(IV) intermediate in biological water oxidation: Spectroscopic signature and a pivot mechanism for water binding. *Chem. Sci.* **2016**, *7*, 72–84. [CrossRef] [PubMed]

36. Ghosh, M.; Singh, K.K.; Panda, C.; Weitz, A.; Hendrich, M.P.; Collins, T.J.; Dhar, B.B.; Sen Gupta, S. Formation of a room temperature stable FeV(O) complex: Reactivity toward unactivated C–H bonds. *J. Am. Chem. Soc.* **2014**, *136*, 9524–9527. [CrossRef] [PubMed]

37. Collins, T.J. TAML oxidant activators: A new approach to the activation of hydrogen peroxide for environmentally significant problems. *Acc. Chem. Res.* **2002**, *35*, 782–790. [CrossRef] [PubMed]

38. Que Jr, L.; Tolman, W.B. Biologically inspired oxidation catalysis. *Nature* **2008**, *455*, 333–340.

39. Nam, W.; Yang, S.J.; Kim, H. Catalytic oxygenation of alkenes and alkanes by oxygen donors catalyzed by cobalt-substituted polyoxotungstate. *Bull. Korean Chem. Soc.* **1996**, *17*, 625–630. [CrossRef]

40. Tang, H.; Shen, C.; Lin, M.; Sen, A. Cobalt porphyrin-catalyzed alkane oxidations using dioxygen as oxidant. *Inorg. Chim. Acta* **2000**, *300–302*, 1109–1111. [CrossRef]

41. Sun, C.; Hu, B.; Liu, Z. Rapid aerobic oxidation of alcohols to carbonyl compounds with dioxygen using metallodeuteroporphyrin dimethyl esters as catalysts in the presence of isobutylaldehyde. *Heteroat. Chem* **2012**, *23*, 295–303. [CrossRef]

42. Nguyen, A.I.; Hadt, R.G.; Solomon, E.I.; Tilley, T.D. Efficient C–H bond activations via O_2 cleavage by a dianionic cobalt(II) complex. *Chem. Sci.* **2014**, *5*, 2874–2878. [CrossRef] [PubMed]

43. Zhou, W.-Y.; Tian, P.; Sun, F.A.; He, M.-Y.; Chen, Q. Highly efficient transformation of alcohol to carbonyl compounds under a hybrid bifunctional catalyst originated from metalloporphyrins and hydrotalcite. *J. Catal.* **2016**, *335*, 105–116. [CrossRef]

44. Zhou, X.; Ji, H. Cobalt porphyrin immobilized on montmorillonite: A highly efficient and reusable catalyst for aerobic oxidation of alcohols to carbonyl compounds. *Chin. J. Catal.* **2012**, *33*, 1906–1912. [CrossRef]

45. Nam, W.; Kim, I.; Kim, Y.; Kim, C. Biomimetic alkane hydroxylation by cobalt(III) porphyrin complex and *m*-chloroperbenzoic acid. *Chem. Commun.* **2001**, *0*, 1262–1263. [CrossRef]

46. Song, Y.J.; Hyun, M.Y.; Lee, J.H.; Lee, H.G.; Kim, J.H.; Jang, S.P.; Noh, J.Y.; Kim, Y.; Kim, S.-J.; Lee, S.J.; et al. Amide-based nonheme cobalt(III) olefin epoxidation catalyst: Partition of multiple active oxidants $Co^V=O$, $Co^{IV}=O$, and Co^{III}-OO(O)CR. *Chem. A Eur. J.* **2012**, *18*, 6094–6101. [CrossRef] [PubMed]

47. Nesterova, O.V.; Kopylovich, M.N.; Nesterov, D.S. Stereoselective oxidation of alkanes with *m*-CPBA as an oxidant and cobalt complex with isoindole-based ligands as catalysts. *RSC Adv.* **2016**, *6*, 93756–93767. [CrossRef]

48. Nurdin, L.; Spasyuk, D.M.; Fairburn, L.; Piers, W.E.; Maron, L. Oxygen–oxygen bond cleavage and formation in Co(II)-mediated stoichiometric O_2 reduction via the potential intermediacy of a Co(IV) oxyl radical. *J. Am. Chem. Soc.* **2018**, *140*, 16094–16105. [CrossRef]

49. Ghosh, A.; Mitchell, D.A.; Chanda, A.; Ryabov, A.D.; Popescu, D.L.; Upham, E.C.; Collins, G.J.; Collins, T.J. Catalase–peroxidase activity of iron(III)−TAML activators of hydrogen peroxide. *J. Am. Chem. Soc.* **2008**, *130*, 15116–15126. [CrossRef]

50. Zhang, R.; Horner, J.H.; Newcomb, M. Laser flash photolysis generation and kinetic studies of porphyrin-manganese-oxo intermediates. Rate constants for oxidations effected by porphyrin-MnV-Oxo species and apparent disproportionation equilibrium constants for porphyrin-MnIV-oxo species. *J. Am. Chem. Soc.* **2005**, *127*, 6573–6582. [CrossRef]

51. Zhang, Z.; Hao, J.; Yang, W.; Lu, B.; Ke, X.; Zhang, B.; Tang, J. Porous Co_3O_4 nanorods-reduced graphene oxide with intrinsic peroxidase-like activity and catalysis in the degradation of methylene blue. *ACS Appl. Mater. Interfaces* **2013**, *5*, 3809–3815. [CrossRef] [PubMed]

52. Kuwabara, J.; Stern, C.L.; Mirkin, C.A. A coordination chemistry approach to a multieffector enzyme mimic. *J. Am. Chem. Soc.* **2007**, *129*, 10074–10075. [CrossRef] [PubMed]

53. Wulff, G. Enzyme-like catalysis by molecularly imprinted polymers. *Chem. Rev.* **2002**, *102*, 1–28. [CrossRef] [PubMed]

54. Li, N.; Lu, W.; Pei, K.; Yao, Y.; Chen, W. Formation of high-valent cobalt-oxo phthalocyanine species in a cellulose matrix for eliminating organic pollutants. *Appl. Catal. B* **2015**, *163*, 105–112. [CrossRef]

55. Afanasiev, P.; Kudrik, E.V.; Albrieux, F.; Briois, V.; Koifman, O.I.; Sorokin, A.B. Generation and characterization of high-valent iron oxo phthalocyanines. *Chem. Commun.* **2012**, *48*, 6088–6090. [CrossRef] [PubMed]

56. Ramdhanie, B.; Telser, J.; Caneschi, A.; Zakharov, L.N.; Rheingold, A.L.; Goldberg, D.P. An example of O_2 binding in a Cobalt(II) corrole system and high-valent cobalt–cyano and cobalt–alkynyl complexes. *J. Am. Chem. Soc.* **2004**, *126*, 2515–2525. [CrossRef] [PubMed]

57. Huang, Z.; Yao, Y.; Lu, J.; Chen, C.; Lu, W.; Huang, S.; Chen, W. The consortium of heterogeneous cobalt phthalocyanine catalyst and bicarbonate ion as a novel platform for contaminants elimination based on peroxymonosulfate activation. *J. Hazard. Mater.* **2016**, *301*, 214–221. [CrossRef]

58. Li, N.; Lu, W.; Pei, K.; Chen, W. Interfacial peroxidase-like catalytic activity of surface-immobilized cobalt phthalocyanine on multiwall carbon nanotubes. *RSC Adv.* **2015**, *5*, 9374–9380. [CrossRef]

59. Li, N.; Wang, Y.; Wu, C.; Lu, W.; Pei, K.; Chen, W. Bioinspired catalytic generation of high-valent cobalt–oxo species by the axially coordinated CoPc on pyridine-functionalized MWCNTs for the elimination of organic contaminants. *Appl. Surf. Sci.* **2018**, *434*, 1112–1121. [CrossRef]

60. Fernández, I.; Pedro, J.R.; Roselló, A.L.; Ruiz, R.; Castro, I.; Ottenwaelder, X.; Journaux, Y. Alcohol oxidation by dioxygen and aldehydes catalysed by square-planar cobalt(III) complexes of disubstituted oxamides and related ligands. *Eur. J. Org. Chem.* **2001**, *2001*, 1235–1247.

61. Li, N.; Zheng, Y.; Jiang, X.; Zhang, R.; Pei, K.; Chen, W. Carbon-based oxamate cobalt(III) complexes as bioenzyme mimics for contaminant elimination in high backgrounds of complicated constituents. *Materials* **2017**, *10*, 1169. [CrossRef] [PubMed]

62. Li, N.; Zheng, Y.; Jiang, X.; Zhang, R.; Chen, W. Generation of reactive cobalt oxo oxamate radical species for biomimetic oxidation of contaminants. *RSC Adv.* **2017**, *7*, 42875–42883. [CrossRef]

63. Winkler, J.R.; Gray, H.B. Electronic Structures of Oxo-Metal Ions. In *Molecular Electronic Structures of Transition Metal Complexes I*; Mingos, D.M.P., Day, P., Dahl, J.P., Eds.; Springer Berlin Heidelberg: Berlin/Heidelberg,Germany, 2012; pp. 17–28.

64. Huang, L.-T.; Ali, A.; Wang, H.-H.; Cheng, F.; Liu, H.-Y. Catalytic oxidation of alkene by cobalt corroles. *J. Mol. Catal. A: Chem.* **2017**, *426*, 213–222. [CrossRef]

65. Betley, T.A.; Wu, Q.; Van Voorhis, T.; Nocera, D.G. Electronic design criteria for O–O bond formation via metal–oxo complexes. *Inorg. Chem.* **2008**, *47*, 1849–1861. [CrossRef] [PubMed]

66. Sala, X.; Romero, I.; Rodríguez, M.; Escriche, L.; Llobet, A. Molecular catalysts that oxidize water to dioxygen. *Angew. Chem. Int. Ed.* **2009**, *48*, 2842–2852. [CrossRef]

67. Romain, S.; Vigara, L.; Llobet, A. Oxygen–oxygen bond formation pathways promoted by ruthenium complexes. *Acc. Chem. Res.* **2009**, *42*, 1944–1953. [CrossRef] [PubMed]

68. Cape, J.L.; Hurst, J.K. Detection and mechanistic relevance of transient ligand radicals formed during [Ru(bpy)$_2$(OH$_2$)]$_2$O^{4+}-catalyzed water oxidation. *J. Am. Chem. Soc.* **2008**, *130*, 827–829. [CrossRef]

69. Niishiro, R.; Takano, Y.; Jia, Q.; Yamaguchi, M.; Iwase, A.; Kuang, Y.; Minegishi, T.; Yamada, T.; Domen, K.; Kudo, A. A CoOx-modified SnNb$_2$O$_6$ photoelectrode for highly efficient oxygen evolution from water. *Chem. Commun.* **2017**, *53*, 629–632. [CrossRef]

70. Zhong, M.; Hisatomi, T.; Kuang, Y.; Zhao, J.; Liu, M.; Iwase, A.; Jia, Q.; Nishiyama, H.; Minegishi, T.; Nakabayashi, M.; et al. Surface modification of CoOx loaded BiVO$_4$ photoanodes with ultrathin p-type NiO layers for improved solar water oxidation. *J. Am. Chem. Soc.* **2015**, *137*, 5053–5060. [CrossRef]

71. Hisatomi, T.; Katayama, C.; Moriya, Y.; Minegishi, T.; Katayama, M.; Nishiyama, H.; Yamada, T.; Domen, K. Photocatalytic oxygen evolution using BaNbO$_2$N modified with cobalt oxide under photoexcitation up to 740 nm. *Energy Environ. Sci.* **2013**, *6*, 3595–3599. [CrossRef]

72. Zecchina, A.; Spoto, G.; Coluccia, S. Surface dioxygen adducts on MgO-CoO solid solutions: Analogy with cobalt-based homogeneous oxygen carriers. *J. Mol. Catal.* **1982**, *14*, 351–355. [CrossRef]

73. Barraclough, C.G.; Lawrance, G.A.; Lay, P.A. Characterization of binuclear. mu.-peroxo and. mu.-superoxo cobalt(III) amine complexes from Raman spectroscopy. *Inorg. Chem.* **1978**, *17*, 3317–3322. [CrossRef]

74. Gerken, J.B.; McAlpin, J.G.; Chen, J.Y.C.; Rigsby, M.L.; Casey, W.H.; Britt, R.D.; Stahl, S.S. Electrochemical water oxidation with cobalt-based electrocatalysts from pH 0–14: The thermodynamic basis for catalyst structure, stability, and activity. *J. Am. Chem. Soc.* **2011**, *133*, 14431–14442. [CrossRef] [PubMed]

75. Takada, K.; Fukuda, K.; Osada, M.; Nakai, I.; Izumi, F.; Dilanian, R.A.; Kato, K.; Takata, M.; Sakurai, H.; Takayama-Muromachi, E.; et al. Chemical composition and crystal structure of superconducting sodium cobalt oxide bilayer-hydrate. *J. Mater. Chem.* **2004**, *14*, 1448–1453. [CrossRef]

76. Amatucci, G.G.; Tarascon, J.M.; Klein, L.C. CoO$_2$, the end member of the Li x CoO$_2$ solid solution. *J. Electrochem. Soc.* **1996**, *143*, 1114–1123. [CrossRef]

77. Motohashi, T.; Katsumata, Y.; Ono, T.; Kanno, R.; Karppinen, M.; Yamauchi, H. Synthesis and properties of CoO$_2$, the x = 0 end member of the LixCoO$_2$ and NaxCoO$_2$ systems. *Chem. Mater.* **2007**, *19*, 5063–5066. [CrossRef]

78. Brunschwig, B.S.; Chou, M.H.; Creutz, C.; Ghosh, P.; Sutin, N. Mechanisms of water oxidation to oxygen: Cobalt(IV) as an intermediate in the aquocobalt(II)-catalyzed reaction. *J. Am. Chem. Soc.* **1983**, *105*, 4832–4833. [CrossRef]

79. Risch, M.; Ringleb, F.; Kohlhoff, M.; Bogdanoff, P.; Chernev, P.; Zaharieva, I.; Dau, H. Water oxidation by amorphous cobalt-based oxides: In situ tracking of redox transitions and mode of catalysis. *Energy Environ. Sci.* **2015**, *8*, 661–674. [CrossRef]

80. Koroidov, S.; Anderlund, M.F.; Styring, S.; Thapper, A.; Messinger, J. First turnover analysis of water-oxidation catalyzed by Co-oxide nanoparticles. *Energy Environ. Sci.* **2015**, *8*, 2492–2503. [CrossRef]

81. Wasylenko, D.J.; Palmer, R.D.; Berlinguette, C.P. Homogeneous water oxidation catalysts containing a single metal site. *Chem. Commun.* **2013**, *49*, 218–227. [CrossRef]

82. Fillol, J.L.; Codolà, Z.; Garcia-Bosch, I.; Gómez, L.; Pla, J.J.; Costas, M. Efficient water oxidation catalysts based on readily available iron coordination complexes. *Nat. Chem.* **2011**, *3*, 807. [CrossRef] [PubMed]

83. Ellis, W.C.; McDaniel, N.D.; Bernhard, S.; Collins, T.J. Fast water oxidation using iron. *J. Am. Chem. Soc.* **2010**, *132*, 10990–10991. [CrossRef] [PubMed]

84. Concepcion, J.J.; Jurss, J.W.; Brennaman, M.K.; Hoertz, P.G.; Patrocinio, A.O.T.; Murakami Iha, N.Y.; Templeton, J.L.; Meyer, T.J. Making oxygen with ruthenium complexes. *Acc. Chem. Res.* **2009**, *42*, 1954–1965. [CrossRef] [PubMed]

85. Hetterscheid, D.G.H.; Reek, J.N.H. Mononuclear water oxidation catalysts. *Angew. Chem. Int. Ed.* **2012**, *51*, 9740–9747. [CrossRef] [PubMed]

86. Sartorel, A.; Bonchio, M.; Campagna, S.; Scandola, F. Tetrametallic molecular catalysts for photochemical water oxidation. *Chem. Soc. Rev.* **2013**, *42*, 2262–2280. [CrossRef] [PubMed]

87. Codolà, Z.; Garcia-Bosch, I.; Acuña-Parés, F.; Prat, I.; Luis, J.M.; Costas, M.; Lloret-Fillol, J. Electronic effects on single-site iron catalysts for water oxidation. *Chem. A Eur. J.* **2013**, *19*, 8042–8047. [CrossRef] [PubMed]

88. Wasylenko, D.J.; Ganesamoorthy, C.; Koivisto, B.D.; Henderson, M.A.; Berlinguette, C.P. Insight into water oxidation by mononuclear polypyridyl Ru catalysts. *Inorg. Chem.* **2010**, *49*, 2202–2209. [CrossRef] [PubMed]

89. Wasylenko, D.J.; Ganesamoorthy, C.; Borau-Garcia, J.; Berlinguette, C.P. Electrochemical evidence for catalyticwater oxidation mediated by a high-valent cobalt complex. *Chem. Commun.* **2011**, *47*, 4249–4251. [CrossRef]

90. Crandell, D.W.; Ghosh, S.; Berlinguette, C.P.; Baik, M.H. How a [Co(IV) a bond and a half O](2+) fragment oxidizes water: Involvement of a biradicaloid [Co(II)-(·O·)](2+) species in forming the O–O bond. *ChemSusChem* **2015**, *8*, 844–852. [CrossRef]

91. Nakazono, T.; Parent, A.R.; Sakai, K. Cobalt porphyrins as homogeneous catalysts for water oxidation. *Chem. Commun.* **2013**, *49*, 6325–6327. [CrossRef]

92. Wang, D.; Groves, J.T. Efficient water oxidation catalyzed by homogeneous cationic cobalt porphyrins with critical roles for the buffer base. *Proc. Natl. Acad. Sci. USA* **2013**, *110*, 15579–15584. [CrossRef] [PubMed]

93. Pizzolato, E.; Natali, M.; Posocco, B.; Montellano López, A.; Bazzan, I.; Di Valentin, M.; Galloni, P.; Conte, V.; Bonchio, M.; Scandola, F.; Sartorel, A. Light driven water oxidation by a single site cobalt salophen catalyst. *Chem. Commun.* **2013**, *49*, 9941–9943. [CrossRef] [PubMed]

94. Brodsky, C.N.; Hadt, R.G.; Hayes, D.; Reinhart, B.J.; Li, N.; Chen, L.X.; Nocera, D.G. In situ characterization of cofacial Co(IV) centers in Co_4O_4 cubane: Modeling the high-valent active site in oxygen-evolving catalysts. *Proc. Natl. Acad. Sci. USA* **2017**, *114*, 3855–3860. [CrossRef] [PubMed]

95. Symes, M.D.; Surendranath, Y.; Lutterman, D.A.; Nocera, D.G. Bidirectional and unidirectional PCET in a molecular model of a cobalt-based oxygen-evolving catalyst. *J. Am. Chem. Soc.* **2011**, *133*, 5174–5177. [CrossRef] [PubMed]

96. Nguyen, A.I.; Ziegler, M.S.; Oña-Burgos, P.; Sturzbecher-Hohne, M.; Kim, W.; Bellone, D.E.; Tilley, T.D. Mechanistic investigations of water oxidation by a molecular cobalt oxide analogue: Evidence for a highly oxidized intermediate and exclusive terminal oxo participation. *J. Am. Chem. Soc.* **2015**, *137*, 12865–12872. [CrossRef] [PubMed]

97. Nguyen, A.I.; Wang, J.; Levine, D.S.; Ziegler, M.S.; Tilley, T.D. Synthetic control and empirical prediction of redox potentials for Co_4O_4 cubanes over a 1.4 V range: Implications for catalyst design and evaluation of high-valent intermediates in water oxidation. *Chem. Sci.* **2017**, *8*, 4274–4284. [CrossRef] [PubMed]

98. Wang, L.-P.; Van Voorhis, T. Direct-coupling O_2 bond forming a pathway in cobalt oxide water oxidation catalysts. *J. Phys. Chem. Lett.* **2011**, *2*, 2200–2204. [CrossRef]

99. Fernando, A.; Aikens, C.M. Reaction pathways for water oxidation to molecular oxygen mediated by model cobalt oxide dimer and cubane catalysts. *J. Phys. Chem. C* **2015**, *119*, 11072–11085. [CrossRef]

100. Li, X.; Siegbahn, P.E.M. Water oxidation mechanism for synthetic Co–Oxides with small nuclearity. *J. Am. Chem. Soc.* **2013**, *135*, 13804–13813. [CrossRef]

101. Mattioli, G.; Giannozzi, P.; Amore Bonapasta, A.; Guidoni, L. Reaction pathways for oxygen evolution promoted by cobalt catalyst. *J. Am. Chem. Soc.* **2013**, *135*, 15353–15363. [CrossRef]

102. Xu, L.; Lei, H.; Zhang, Z.; Yao, Z.; Li, J.; Yu, Z.; Cao, R. The effect of the trans axial ligand of cobalt corroles on water oxidation activity in neutral aqueous solutions. *Phys. Chem. Chem. Phys.* **2017**, *19*, 9755–9761. [CrossRef] [PubMed]

103. Pfaff, F.F.; Kundu, S.; Risch, M.; Pandian, S.; Heims, F.; Pryjomska-Ray, I.; Haack, P.; Metzinger, R.; Bill, E.; Dau, H.; et al. An oxocobalt(IV) complex stabilized by lewis acid interactions with scandium(III) ions. *Angew. Chem. Int. Ed.* **2010**, *50*, 1711–1715. [CrossRef] [PubMed]

104. Hong, S.; Pfaff, F.F.; Kwon, E.; Wang, Y.; Seo, M.-S.; Bill, E.; Ray, K.; Nam, W. Spectroscopic capture and reactivity of a low-spin cobalt(IV)–oxo complex stabilized by binding redox-inactive metal ions. *Angew. Chem.* **2014**, *126*, 10571–10575. [CrossRef]

105. Wang, B.; Lee, Y.-M.; Tcho, W.-Y.; Tussupbayev, S.; Kim, S.-T.; Kim, Y.; Seo, M.S.; Cho, K.-B.; Dede, Y.; Keegan, B.C.; et al. Synthesis and reactivity of a mononuclear non-haem cobalt(IV)–oxo complex. *Nat. Commun.* **2017**, *8*, 14839. [CrossRef] [PubMed]

106. Liu, H.-Y.; Yam, F.; Xie, Y.-T.; Li, X.-Y.; Chang, C.K. A bulky bis-pocket manganese(V)−oxo corrole complex: Observation of oxygen atom transfer between triply bonded $Mn^V \equiv O$ and alkene. *J. Am. Chem. Soc.* **2009**, *131*, 12890–12891. [CrossRef] [PubMed]

107. Hong, S.; So, H.; Yoon, H.; Cho, K.-B.; Lee, Y.-M.; Fukuzumi, S.; Nam, W. Reactivity comparison of high-valent iron(IV)–oxo complexes bearing *N*-tetramethylated cyclam ligands with different ring size. *Dalton Trans.* **2013**, *42*, 7842–7845. [CrossRef] [PubMed]

108. Goetz, M.K.; Hill, E.A.; Filatov, A.S.; Anderson, J.S. Isolation of a terminal Co(III)–oxo complex. *J. Am. Chem. Soc.* **2018**, *140*, 13176–13180. [CrossRef] [PubMed]